Materials Chemistry and Physics 281 (2022) 125869

Contents lists available at ScienceDirect

Materials Chemistry and Physics

journal homepage: www.elsevier.com/locate/matchemphys

Ca_2C MXene monolayer as a superior material for detection of toxic pnictogen hydrides

Yunrui Yan [a,*], Zhang Wei [b]

[a] Department of Material Science and Nanoengineering, Rice University, Houston, USA
[b] College of Chemistry and Molecular Engineering, Peking University, Beijing, 100871, China

HIGHLIGHTS

- The DFT study on the adsorption of pnictogen hydrides on Ca_2C MXene layer.
- Adsorption of NH_3 on the Ca_2C MXene was the strongest among the studied gases.
- The molecular dynamics calculations confirmed the thermal stability of the gas/MXene systems.

ARTICLE INFO

Keywords:
Ca_2C
MXene
Pnictogen hydrides
Gas sensor
Density functional theory

ABSTRACT

Carbide-nitride MXene two-dimensional materials have great potential to be used in the future electronic applications. However, determining the interaction between gas molecules and two-dimensional materials is an important step for designing novel gas sensors. Herein, we theoretically investigate the sensitivity of Ca_2C MXene monolayer toward pnictogen hydrides (NH_3, PH_3, AsH_3, and SbH_3). We found that the toxic gas molecules adsorption with high adsorption energies have a considerable effect on the electronic properties of the Ca_2C MXene layer. The molecular dynamics calculations at 400 K also verified the thermal stability of the gas/Ca_2C systems. Our results might be helpful for future researches toward application of carbide-nitride MXene materials for detecting toxic gas molecules.

1. Introduction

Two-dimensional (2D) nanomaterials attracted a wide attentions due to their divers applications such as sensing devices, catalysis, optoelectronic applications, and medicine [1–4]. Besides, there have been many studies on a new class of 2D materials, carbide-nitride (MXenes), with interesting properties [5–8]. MXenes are also successfully synthesized by the elements of group IIIA or IVA and a carbon or nitrogen. Similar to the 2D transition metal dichalcogenides, MXenes can be semiconducting or metallic [9–15]. Furthermore, these novel 2D MXene materials possess high metallic conductivity [16,17]. High performance of the 2D MXene layers have been verified in divers fields such as bio-sensors [18] and hydrogen storage applications [19–24]. For instance, Liu et al. [25, 26] investigated the application of 2D Ti_3C_2 in the hydrogen sorption behavior of MgH_2. Motivated by the successful synthesis [27] of the 2D MXene monolayer with calcium carbide composition (Ca_2C), in this work we investigate the application of the Ca_2C monolayer as adsorbent for use in next generation pnictogen hydrides (PHs) sensor. While the interesting properties of the considered Ca_2C MXene attract high attentions, research on the applications of the considered 2D material to detect toxic PHs are still scarce.

Detecting toxic environmental pollutants is an important issue relating to human life. Accordingly, the design of high-efficient gas sensors has been attracted much attention. Detection of toxic PHs, (NH_3, PH_3, AsH_3, and SbH_3) using nanomaterials have been previously investigated [28–41]. NH_3, a volatile substance with a low boiling point, despite the harmful of this gas, it is applied in various synthesizing procedures [42,43]. PH_3, as a extremely toxic agent, effects the central nervous network and lungs [44–46]. As another toxic PH, some studies have been performed on the detection of AsH_3 [33,37]. While diverse nanomaterials have been proposed to detect of PHs [28–41], it has not been carried out a comprehensive research to detect the PHs using Ca_2C MXene monolayer. Previous fascinating findings [18–27] have inspired us to explore the application of Ca2C MXene monolayer as the gas sensor

* Corresponding author.
E-mail address: yrui9916@gmail.com (Y. Yan).

https://doi.org/10.1016/j.matchemphys.2022.125869
Received 30 August 2021; Received in revised form 9 February 2022; Accepted 14 February 2022
Available online 15 February 2022

to detect toxic PHs. So, this work is conducted to investigate the performance of Ca_2C MXene layer to detect toxic NH_3, PH_3, AsH_3, and SbH_3, using density functional theory (DFT) calculations.

2. Computational details

All calculations of the Ca_2C MXene as well as PH/Ca_2C complexes were performed using GAUSSIAN09 package [47]. We have carried out the optimization of the considered MXenes by nine DFT functionals [48]: PBE [49], TPSS [50], BP86 [51,52], B3LYP [53,54], TPSSh [55], PBE0 [56], CAM-B3LYP [57], M11 [58], and LC-WPBE [59]. Our results reveal an good agreement with previously measured electronic properties of the Ca_2C MXene layer [27] and PBE DFT method. Accordingly, the PBE functional is chosen in our study to calculate the properties of the MXene and PH/MXene complexes. The van der Waals (vdW) bindings are also computed using the DFT-D3 technique [60]. The stability of the PH/MXene complexes was also examined by frequency calculations. Besides, cohesive energy (E_{coh}) of the MXene layer was computed using by:

$$E_{coh} = \left(E_{tot} - \sum_i n_i E_i\right) \Big/ j \quad (1)$$

The adsorption energy (E_{ads}) can be also calculated by:

$$E_{ads} = E_{complex} - E_{PH} - E_{MXene} \quad (2)$$

Finally, charge transfer between PHs and MXene layer was calculated using the natural bond orbital (NBO) approach [61,62].

3. Result and discussions

3.1. Ca_2C MXene monolayer

Ca_2C MXene monolayers have the hexagonal symmetry, in which the C atom is located between two Ca atoms, as shown in Fig. 1.

Fig. 1 represents the optimized geometry of the MXene with the average Ca–C 2.63 Å and Ca–Ca 3.40 Å bond lengths, and Ca–Ca–C (49°), Ca–C–Ca (81), and C–Ca–C (99°) angles which are in agreement with the previous studies [63,64]. The thermal stability of the MXene monolayer with *D2h* symmetry, has been recently confirmed by using molecular dynamics calculations [65]. No imaginary frequencies were obtained, representing that the MXene layer is dynamically stable and belongs to minima in the potential energy surface. The calculated cohesive energy for the Ca_2C MXene monolayer is −3.95 eV, that is in agreements with the previous study [66]. Note that, the cohesive energy is between the values of already synthesized 2D systems such as graphene (−7.90 eV) [67] and silicene (−4.01 eV) [68]. Our calculations also reveal that the HOMO-LUMO energy gap (E_{gap}) of the Ca_2C is 0.21 eV, offering the Ca_2C MXene monolayer should present metallic nature, that is in agreements with the previous studies [64,65]. To verify the electronic structure of MXene monolayer, the corresponding density of state (DOS) are analyzed and presented in Fig. 1 (c). As shown in this figure, the metallic nature of considered layer has been verified with DOS analysis.

3.2. PH@MXene complexes

We investigate the adsorption of a PH gas molecule on the surface of Ca_2C layer. Structurally, 5 adsorption positions are found on the Ca_2C layer, such as on top of Ca atoms, Ca–C and Ca–Ca bonds, hexagonal and rhombuses hollows of Ca_2C sheet. After full optimization without any constrain, the configurations with the adsorbed XH_3 gas molecules with X head to the Ca atom of the Ca_2C monolayer was found to be the most stable adsorption configurations (Fig. 2).

It is worth to mention that other initial adsorption configurations were reoriented to the stable configuration. The calculated parameters such as interaction distance (r), adsorption energy (E_{ads}), HOMO-LUMO gap energy (E_{gap}), and total charge transfer (Q_T) for the considered PH/Ca_2C complexes are reported in Table 1.

The X … Ca interaction distances (r) are equal to 2.00, 2.50, 2.80, and 3.00 Å, for NH_3/Ca_2C, PH_3/Ca_2C, AsH_3/Ca_2C, and SbH_3/Ca_2C, respectively. The lowest interaction distance was obtained from the N… Ca interaction for the NH_3/Ca_2C complex. As reported in Table 1, the NH_3 molecule was adsorbed over the surface of Ca_2C with the adsorption energy (E_{ads}) of −1.36 eV. E_{ads} values for PH_3/Ca_2C, AsH_3/Ca_2C, and SbH_3/Ca_2C systems are −1.10, −0.82, and −0.56 eV, respectively. The calculated E_{ads} here are in range of measured E_{ads} values of PH gas molecules adsorbed on various adsorbents [65]. The calculated NBO charges over the adsorbed NH_3, PH_3, AsH_3, and SbH_3 gas molecules are 195 |me|, 180 |me|, 104 |me|, and 76 |me|, respectively. As results show, charge transfers occur from PH gas molecules to $C_{a2}C$ MXene. The calculated E_{gap} values for PH/Ca_2C systems, are 0.62, 0.59, 0.43, and

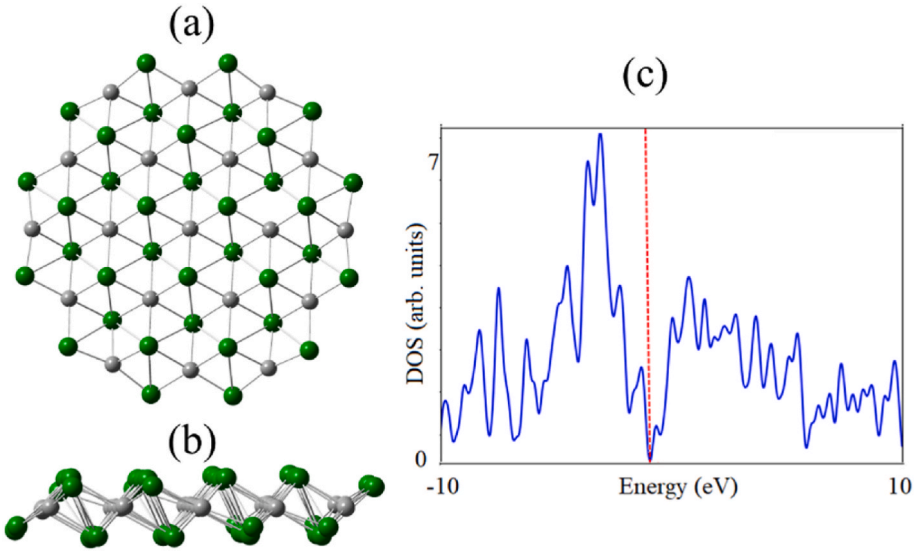

Fig. 1. Top (a) and side (b) views and the density of state diagram (c) of optimized Ca_2C MXene monolayer. The Ca and C atoms are shown in green and gray colors, respectively. Hydrogen is used as passivated atom on the periphery, which is not shown. (For interpretation of the references to color in this figure legend, the reader is referred to the Web version of this article.)

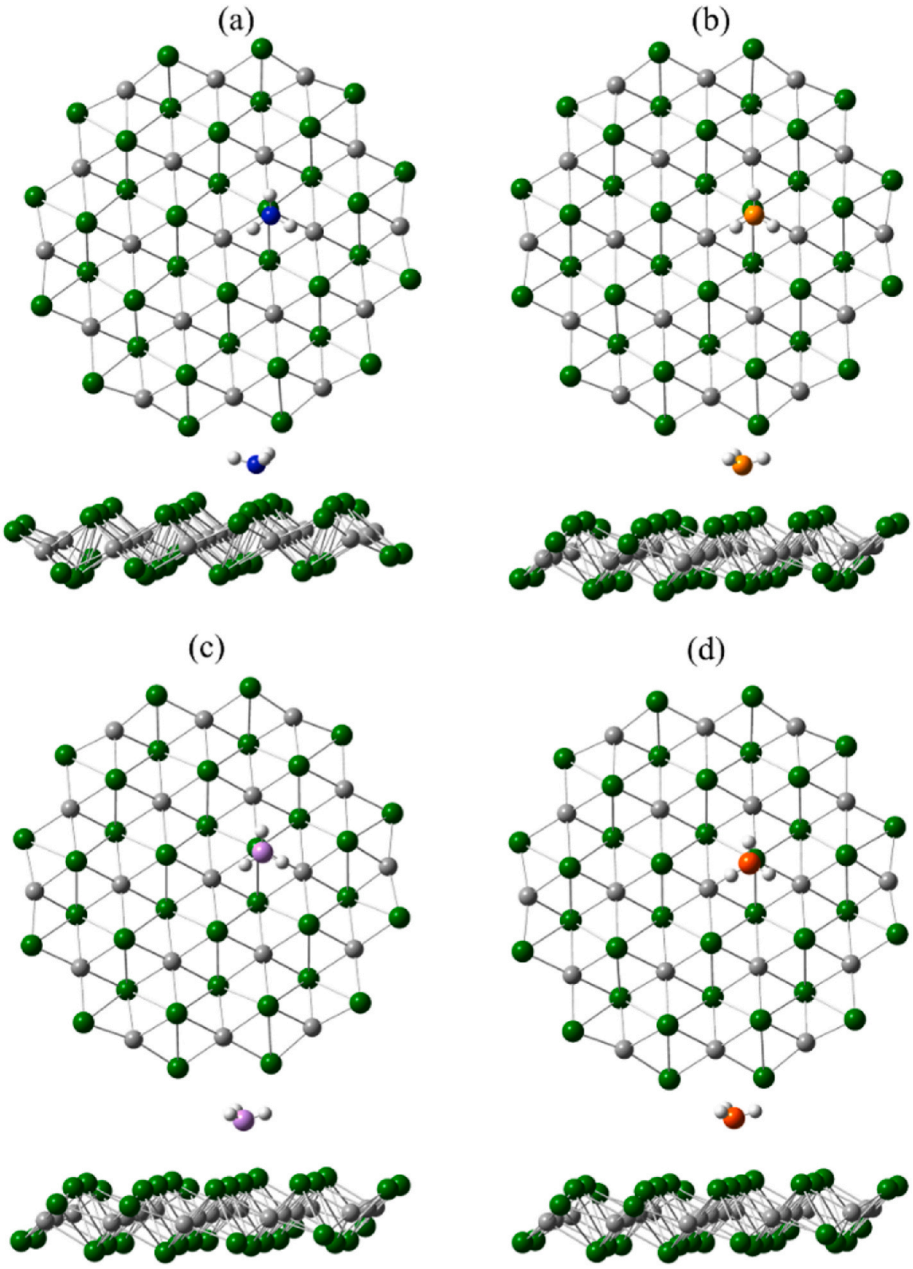

Fig. 2. Top and side views of optimized NH_3/Ca_2C (a), PH_3/Ca_2C (b), AsH_3/Ca_2C (c), and SbH_3/Ca_2C complexes. The Ca, C, H, N, As, and Sb atoms are shown in green, gray, white, blue, brown, and orang colors, respectively. Hydrogen is used as passivated atom on the periphery, which is not shown. (For interpretation of the references to color in this figure legend, the reader is referred to the Web version of this article.)

Table 1
The calculated interaction distance (r), adsorption energy (E_{ads}), HOMO-LUMO energy gap (E_{gap}), change in the E_{gap} of Ca_2C upon the adsorption process (%ΔE_{gap}), and total charge transfer (Q_T) for the considered PH/Ca_2C systems.

system	r (Å)	E_{ads} (eV)	Q_T (|me|)	E_{gap} (eV)	%ΔE_{gap}
Ca_2C	–	–	–	0.21	–
NH_3/Ca_2C	2.00	−1.36	185	0.62	195
PH_3/Ca_2C	2.50	−1.10	172	0.59	180
AsH_3/Ca_2C	2.80	−0.82	102	0.43	104
SbH_3/Ca_2C	3.00	−0.56	72	0.37	76

0.37 eV for the NH_3/Ca_2C, PH_3/Ca_2C, AsH_3/Ca_2C, and SbH_3/Ca_2C systems, respectively. To verify the effect of PH gas molecules on the electronic properties of the Ca_2C MXene, the corresponding density of states (DOS) are plotted and represented in Fig. 3.

Consistent with the obtained energetic analyses, the DOS analysis also determines that the interactions between NH_3 and PH_3 gas molecules and Ca_2C are stronger than the AsH_3 and SbH_3 molecules. As represented from Fig. 3, the strong interaction causes a significant change of the DOS on both sides near the Fermi level. For all of the NH_3/Ca_2C, PH_3/Ca_2C, AsH_3/Ca_2C, and SbH_3/Ca_2C complexes, valence and conduction levels shift to lower and higher energies, respectively, leading to significant enhancement of the MXene's E_{gap}. The %ΔE_{gap} values for these PH/MXene systems are 195, 180, 104, and 76%, respectively. However, the larger changes in the E_{gap} values shows higher sensitivity of the Ca_2C toward the NH_3 and PH_3 compared to the AsH_3 and SbH_3 adsorption. This observation is anticipated to bring about clear modification in the electrical conductivity of Ca_2C according to the following formula [69].

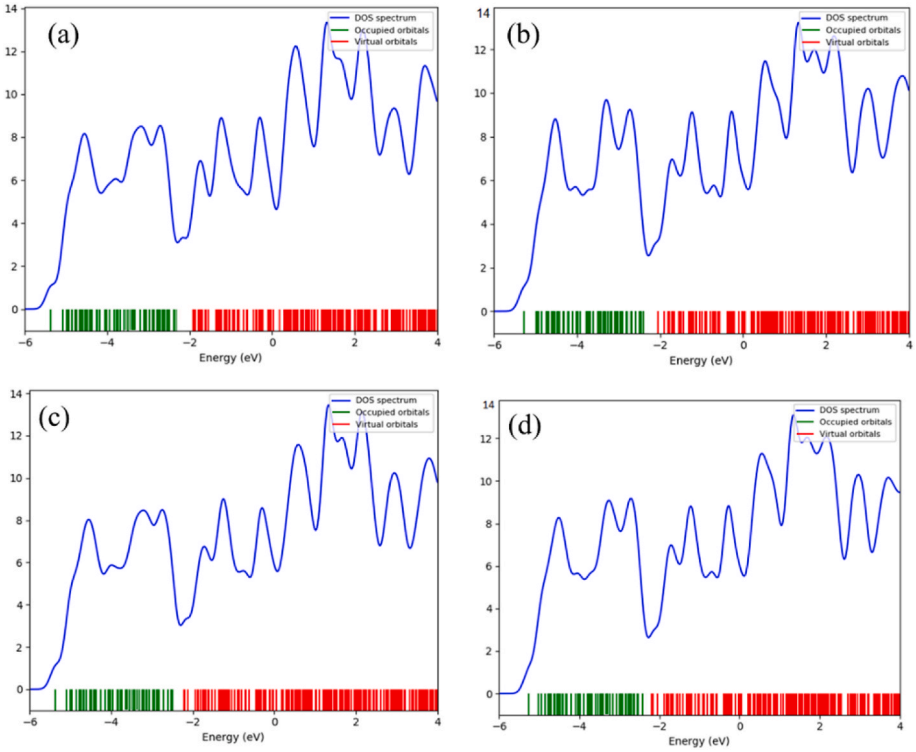

Fig. 3. The DOS analysis of the NH_3/Ca_2C (a), $PH3_2/Ca_2C$ (b), AsH_3/Ca_2C (c), and SbH_3/Ca_2C complexes.

$$\sigma \propto \exp\left(\frac{-E_{gap}}{2kT}\right) \quad (3)$$

where σ is the electrical conductivity and k is the Boltzmann's constant. So, considerable enhances of about 195 and 180% in the E_{gap} value for NH_3/Ca_2C and PH_3/Ca_2C complexes determine the high sensitivity of the electronic properties of Ca_2C toward the NH_3 and PH_3 gas molecules.

Now, we compute the recovery time (τ) under a specific temperature to estimate the possibility of adsorption od considered PH gas molecules. If the E_{ads} is remarkably enhance4d, much longer τ is predicted based on the conventional transition state rule [70]:

$$\tau = \nu_0^{-1} \exp\left(\frac{-E_{ads}}{kT}\right) \quad (4)$$

The υ_0, k, and T indicate the attempt frequency, Boltzmann's constant, and temperature, respectively (υ_0~800 THz). Enhancing E_{ads}, the necessary T for desorption increases, and subsequently, the τ becomes longer. The calculated τ for considered PH gas molecule desorption is reported in Table 2.

Our results show that the calculated τ values are in the range [71] that is appropriate for sensing NH_3 and PH_3 at 400 K and AsH_3 and SbH_3 at 300 K.

The molecular dynamics (MD) calculations in the NVT ensemble, with a time step of 1 fs in 5000 with a massive GGM thermostat, has been also carried out at 400 K to investigate thermal stability of studied systems (Fig. 4).

The results confirmed the thermal stability of the pristine Ca_2C MXene and the NH_3/Ca_2C and PH_3/Ca_2C complexes at 400 K. We found that the changes in the total energy that are criteria for the thermal stability of considered structures are ignorable.

Now, it remains to investigate the humidity interference of the Ca_2C MXene by exposing it to the water. The humidity interference is an important parameter for designing the gas detecting materials. Divers orientations of the H_2O adsorption on the Ca_2C MXene were examined. After full structural optimization without any constrain, the configuration with the adsorbed H_2O with O head to the Ca atom of the Ca2C monolayer was found to be the most stable adsorption configuration. The calculated interaction distance and E_{ads} of the H_2O/Ca_2C systems are 2.25 Å and −0.89 eV, respectively, which is lower than NH_3/Ca_2C and $PH_3/Ca2C$ systems. It should be noted that the E_{ads} values of the H_2O/Ca_2C is relatively more negative than AsH_3/Ca_2C and SbH_3/Ca_2C systems. The $\%\Delta E_{gap}$ of H_2O/Ca_2C system is +88%, while this parameter for the NH_3/Ca_2C, PH_3/Ca_2C, AsH_3/Ca_2C, and SbH_3/Ca_2C systems are 195%, 180%, 104%, 76%, respectively. Thus, the pure Ca_2C MXene has a more electronic sensitivity to the H_2O molecule as compared to the NH_3, PH_3, and AsH_3 gas molecules. In this respect, the Ca_2C MXene may detect NH_3, PH_3, and AsH_3 gas molecules in the presence of H_2O.

Table 2
Calculated τ (sec) for the considered PH/MXene complexes.

system	τ (300k)	τ(400k)
NH_3/Ca_2C	8.79×10^{7}	1.71×10^{2}
PH_3/Ca_2C	3.77×10^{3}	9.04×10^{-2}
AsH_3/Ca_2C	7.45×10^{-2}	2.68×10^{-5}
SbH_3/Ca_2C	3.20×10^{-6}	1.48×10^{-5}

4. Conclusions

In summary, we performed DFT calculations to investigate the adsorption of PHs such as NH_3, PH_3, AsH_3, and SbH_3 gas molecules on the Ca_2C MXene. The considered toxic gas molecules are chemically adsorbed on the Ca_2C via the adsorption configurations of Ca atom of the Ca_2C and X atom of the XH_3 (NH_3, PH_3, AsH_3, and SbH_3)gas molecules, with adsorption energies in range of −0.56 eV to −1.36 eV. The ΔE_{gap} of the Ca_2C MXene has been increased from 76% % to 195% due to the strong interactions between HP and MXene monolayer. These results reveal that the Ca_2C MXene can be a used as an appropriate adsorbent to detect harmful PH gas molecules. The results of the present work are important findings because reveal the performance of novel 2D nanomaterials based on Ca_2C MXene in gas sensor applications.

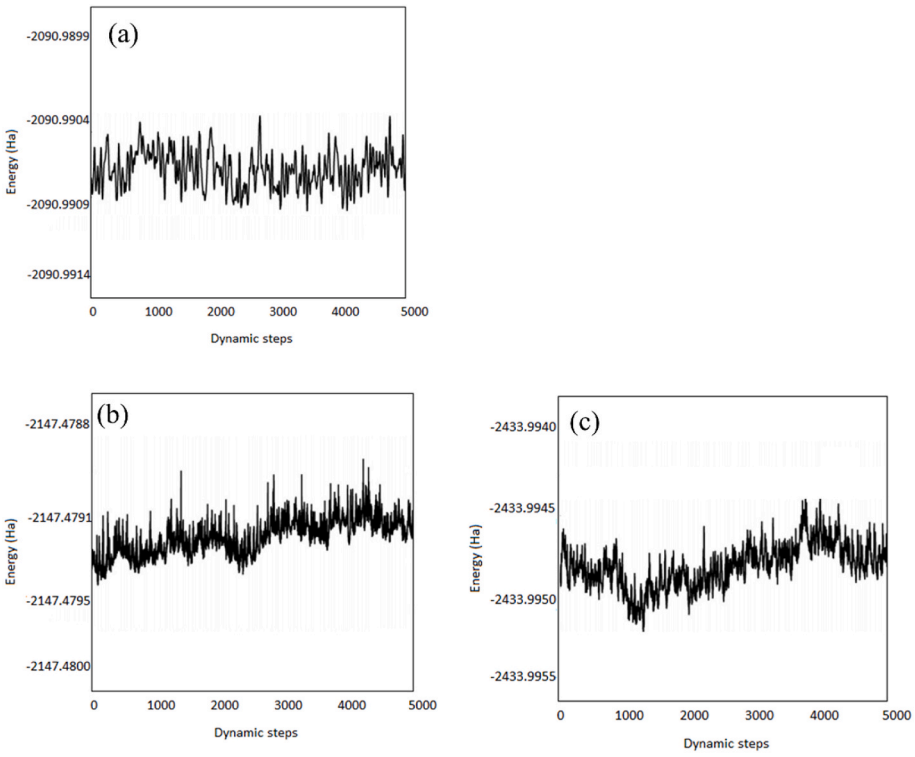

Fig. 4. The MD calculations at 400 K for the (a) pristine Ca_2C monolayer, (b) NH_3/Ca_2C, and (c) PH_3/Ca_2C complexes.

CRediT authorship contribution statement

Yunrui Yan: Supervision, Resources, Project administration, Writing – review & editing. **Zhang Wei:** Writing – review & editing.

Declaration of competing interest

The authors declare that they have no known competing financial interests or personal relationships that could have appeared to influence the work reported in this paper.

Acknowledgments

The authors are grateful to Peking University for computational resources and financial supports.

References

[1] Y.P. Guo, Y.Q. Wei, H.Q. Li, T.Y. Zhai, Layer structured materials for advanced energy storage and conversion, Small 13 (2017), 1701649.
[2] A. Omidvar, Charge-controlled switchable CO adsorption on FeN 4 cluster embedded in graphene, Surf. Sci. 668 (2018) 117–124.
[3] A. Omidvar, Electronic structure tuning and band gap opening of nitrogen and boron doped holey graphene flake: the role of single/dual doping, Mater. Chem. Phys. 202 (2017) 258–265.
[4] A. Omidvar, Borophene: a novel boron sheet with a hexagonal vacancy offering high sensitivity for hydrogen cyanide detection, Comput. Theor. Chem. 1115 (2017) 179–184.
[5] J. Zhu, E.N. Ha, G.L. Zhao, Y. Zhou, D.S. Huang, G.Z. Yue, L.S. Hu, N. Sun, Y. Wang, L.Y.S. Lee, C. Xu, K.Y. Wong, D. Astruc, P.X. Zhao, Recent advance in MXenes: a promising 2D material for catalysis, sensor and chemical adsorption, Coord. Chem. Rev. 352 (2017) 306–327.
[6] M. Naguib, M. Kurtoglu, V. Presser, J. Lu, J. Niu, M. Heon, L. Hultman, Y. Gogotsi, M.W. Barsoum, Two-dimensional nanocrystals produced by exfoliation of Ti3AlC2, Adv. Mater. 23 (2011) 4248–4253.
[7] M. Naguib, O. Mashtalir, J. Carle, V. Presser, J. Lu, L. Hultman, Y. Gogotsi, M. W. Barsoum, Two-dimensional transition metal carbides, ACS Nano 6 (2012) 1322–1331.
[8] F. Chang, C. Li, J. Yang, H. Tang, M. Xue, Synthesis of a new graphene-like transition metal carbide by de-intercalating Ti3AlC2, Mater. Lett. 109 (2013) 295–298.
[9] H. Lin, X. Wang, L. Yu, Y. Chen, J. Shi, Two-dimensional ultrathin MXene ceramic nanosheets for photothermal conversion, Nano Lett. 17 (2017) 384–391.
[10] M.R. Lukatskaya, O. Mashtalir, C.E. Ren, Y. Dall'Agnese, P. Rozier, P.L. Taberna, Y. Gogotsi, Cation intercalation and high volumetric capacitance of two-dimensional titanium carbide, Science 341 (2013) 1502–1505.
[11] L. Ding, Y. Wei, Y. Wang, H. Chen, J. Caro, H. Wang, A two-dimensional lamellar membrane: MXene nanosheet stacks, Angew. Chem. Int. Ed. 56 (2017) 1825–1829.
[12] S.J. Kim, H.J. Koh, C.E. Ren, O. Kwon, K. Maleski, S.Y. Cho, H.T. Jung, Metallic Ti3C2T x MXene gas sensors with ultrahigh signal-to-noise ratio, ACS Nano 12 (2018) 986–993.
[13] X. Xie, S. Chen, W. Ding, Y. Nie, Z. Wei, An extraordinarily stable catalyst: Pt NPs supported on two-dimensional Ti3C2X2 (X = OH, F) nanosheets for oxygen reduction reaction, Chem. Commun. 49 (2013) 10112–10114.
[14] H. Lin, Y. Chen, J. Shi, Insights into 2D MXenes for versatile biomedical applications: current advances and challenges ahead, Adv. Sci. 5 (2018), 1800518.
[15] H. Lin, Y. Wang, S. Gao, Y. Chen, J. Shi, Theranostic 2D tantalum carbide (MXene), Adv. Mater. 30 (2018), 1703284.
[16] S.J. Kim, H.-J. Koh, C.E. Ren, O. Kwon, K. Maleski, S.-Y. Cho, B. Anasori, C.-K. Kim, Y.-K. Choi, J. Kim, Y. Gogotsi, H.-T. Jung, Metallic Ti3C2Tx MXene gas sensors with ultrahigh signal-tonoise ratio, ACS Nano 12 (2018) 986–993.
[17] N. Driscoll, A.G. Richardson, K. Maleski, B. Anasori, O. Adewole, P. Lelyukh, L. Escobedo, D.K. Cullen, T.H. Lucas, Y. Gogotsi, F. Vitale, Two-dimensional Ti3C2 MXene for highresolution neural interfaces, ACS Nano 12 (2018) 10419–10429.
[18] A. Sinha, H. Dhanjai, H. Zhao, Y. Huang, X. Lu, J. Chen, R. Jain, An emerging material for sensing and biosensingr, Trends Anal. Chem. 105 (2018) 424–435.
[19] A. Omidvar, Reversible hydrogen adsorption on Co/N4 cluster embedded in graphene: the role of charge manipulation, Chem. Phys. 493 (2017) 85–90.
[20] G. Chen, Y. Zhang, H. Cheng, Y.F. Zhu, L.Q. Li, H.J. Lin, Effects of two-dimension MXene Ti 3C2 on hydrogen storage performances of MgH2–LiAlH4 composite, Chem. Phys. 522 (2019) 178–187.
[21] J.X. Li, S. Wang, Y.L. Du, W.H. Liao, Catalytic effect of Ti2C MXene on the dehydrogenation of MgH2, Int. J. Hydrogen Energy 44 (2019) 6787–6794.
[22] K. Xian, M. Gao, Z. Li, J. Gu, Y. Shen, S. Wang, Z. Yao, Y. Liu, H. Pan, Superior kinetic and cyclic performance of a 2D titanium carbide incorporated 2LiH + MgB2 composite toward highly reversible hydrogen storage, ACS Appl. Energy Mater. 2 (2019) 4853–4864.
[23] L. Zang, W.Y. Sun, S. Liu, Y.K. Huang, H.T. Yuan, Z.L. Tao, Y.J. Wang, Enhanced hydrogen storage properties and reversibility of LiBH4 confined in two-dimensional Ti3C2, ACS Appl. Mater. Interfaces 10 (2018) 19598–19604.
[24] Y.P. Fan, Z.L. Yuan, G.D. Zou, Q.R. Zhang, B.Z. Liu, Q.M. Peng, Two-dimensional MXene/A-TiO2 composite with unprecedented catalytic activation for sodium alanate, Catal. Today 318 (2018) 167–174.
[25] Y. Liu, H. Du, X. Zhang, Y. Yang, M. Gao, H. Pan, Superior catalytic activity derived from a two-dimensional Ti3C2 precursor towards the hydrogen storage reaction of magnesium hydride, Chem. Commun. 52 (2016) 705–708.

[26] H. Gao, Y. Liu, Y. Zhu, J. Zhang, L. Li, Catalytic effect of sandwich-like Ti3C2/TiO2 (A)-C on hydrogen storage performance of MgH2, Nanotechnology 31 (2019), 115404.
[27] Y.L. Li, S.N. Wang, A.R. Oganov, H. Gou, J.S. Smith, T.A. Strobel, Investigation of exotic stable calcium carbides using theory and experiment, Nat. Commun. 6 (2015) 1–9.
[28] R. Miotto, G.P. Srivastava, R.H. Miwa, A.C. Ferraz, A comparative study of dissociative adsorption of NH 3, PH 3, and AsH 3 on Si (001)–(2× 1), J. Chem. Phys. 21 (2001) 9549–9556.
[29] P. Buasaeng, W. Rakrai, B. Wanno, C. Tabtimsai, DFT investigation of NH3, PH3, and AsH3 adsorptions on Sc-, Ti-, V-, and Cr-doped single-walled carbon nanotubes, Appl. Surf. Sci. 400 (2017) 506–514.
[30] S.M. Aghaei, M.M. Monshi, I. Torres, S.M. Zeidi, I. Calizo, DFT study of adsorption behavior of NO, CO, NO2, and NH3 molecules on graphene-like BC3: a search for highly sensitive molecular sensor, Appl. Surf. Sci. 427 (2018) 326–333.
[31] J.M. Jasmine, A. Aadhityan, D.J. Thiruvadigal, A first-principles study of Cl2, PH3, AsH3, BBr3 and SF4 gas adsorption on MoS2 monolayer with S and Mo vacancy, Appl. Surf. Sci. 489 (2019) 841–848.
[32] V. Kumar, D.R. Roy, Single-layer stanane as potential gas sensor for NO2, SO2, CO2 and NH3 under DFT investigation, Phys. E 110 (2019) 100–106.
[33] J. Arasteh, M. Naseh, DFT study of arsine (AsH3) gas adsorption on pristine, Stone-Wales-defected, and Fe-doped single-walled carbon nanotubes, Struct. Chem. 1 (2019) 97–105.
[34] A. Bafekry, M. Ghergherehchi, S.F. Shayesteh, F.M. Peeters, Adsorption of molecules on C3N nanosheet: a first-principles calculations, Chem. Phys. 526 (2019), 110442.
[35] Y. Yong, H. Cui, Q. Zhou, X. Su, Y. Kuang, X. Li, C2N monolayer as NH3 and NO sensors: a DFT study, Appl. Surf. Sci. 487 (2019) 488–495.
[36] S. Larki, E. Shakerzadeh, E.C. Anota, R. Behjatmanesh-Ardakani, The Al, Ga and Sc dopants effect on the adsorption performance of B12N12 nanocluster toward pnictogen hydrides, Chem. Phys. 526 (2019), 110424.
[37] Y. Li, X. Sun, L. Zhou, P. Ning, L. Tang, Density functional theory analysis of selective adsorption of AsH 3 on transition metal-doped graphene, J. Mol. Model. 5 (2019) 145.
[38] R. Bhuvaneswari, V. Nagarajan, R. Chandiramouli, Arsenene nanoribbons for sensing NH3 and PH3 gas molecules–a first-principles perspective, Appl. Surf. Sci. 469 (2019) 173–180.
[39] V.A. Ranea, P.L. Quiña, N.M. Yalet, General adsorption model for H2S, H2Se, H2Te, NH3, PH3, AsH3 and SbH3 on the V2O5 (0 0 1) surface including the van der Waals interaction, Chem. Phys. Lett. 720 (2019) 58–63.
[40] F. Safari, M. Moradinasab, M. Fathipour, H. Kosina, Adsorption of the NH3, NO, NO2, CO2, and CO gas molecules on blue phosphorene: a first-principles study, Appl. Surf. Sci. 464 (2019) 153–161.
[41] F. Mofidi, A. Reisi-Vanani, Investigation of the electronic and structural properties of graphyne oxide toward CO, CO2 and NH3 adsorption: a DFT and MD study, Appl. Surf. Sci. 507 (2020) 145134.
[42] Don M. Yost, Don M. Yost: Systematic Inorganic Chemistry. READ BOOKS, 2007, Kirja Googlen teoshaussa, 2007, ISBN 1406773026 (englanniksi).
[43] L. Perry, L. Dale, Handbook of Inorganic Compounds, CRC Press, 1995.
[44] B. Berck, Sorption of phosphine by cereal products, J. Agric. Food Chem. 16 (1968) 419–425.
[45] S.D. Gokhale, W.L. Jolly, Phosphine, Inorg. Synth. 9 (1967) 56–58.
[46] G. Gassmann, J.E.E. van Beusekom, D. Glindemann, Naturwissenschaften 83 (1996) 129–131.
[47] M.J. Frisch, et al., Gaussian 09, Revision A.02, Gaussian, Inc., Wallingford, CT, 2009.
[48] A. Omidvar, Defective carbon nanocone as an anode material for lithium-ion batteries, ACS Appl. Energy Mater. 3 (2020) 11463–11469.
[49] J.P. Perdew, K. Burke, M. Ernzerhof, Generalized gradient approximation made simple, Phys. Rev. Lett. 77 (1996) 3865–3868.
[50] J. Tao, J.P. Perdew, V.N. Staroverov, G.E. Scuseria, Climbing the density functional ladder: nonempirical meta-generalized gradient approximation designed for molecules and solids, Phys. Rev. Lett. 91 (2003) 146401-1–146401-4.
[51] A.D. Becke, Density-functional exchange-energy approximation with correct asymptotic behavior, Phys. Rev. A 38 (1988) 3098–3100.
[52] J.P. Perdew, Density-functional approximation for the correlation energy of the inhomogeneous electron gas, Phys. Rev. B 33 (1986) 8822–8824.
[53] A.D. Becke, Density-functional thermochemistry. III. The role of exact exchange, J. Chem. Phys. 98 (1993) 5648–5652.
[54] C. Lee, W. Yang, R.G. Parr, Development of the colle-salvetti correlation-energy formula into a functional of the electron density, Phys. Rev. B 37 (1988) 785–789.
[55] M. Ernzerhof, J.P. Perdew, Generalized gradient approximation to the angle- and system-averaged exchange hole, J. Chem. Phys. 109 (1998) 3313–3320.
[56] A.D. Boese, J.M.L. Martin, Development of density functionals for thermochemical kinetics, J. Chem. Phys. 121 (2004) 3405–3416.
[57] T. Yanai, D.P. Tew, N.C. Handy, A new hybrid exchange-correlation functional using the coulomb-attenuating method (CAM-B3LYP), Chem. Phys. Lett. 393 (2004) 51–57.
[58] R. Peverati, D.G. Truhlar, Improving the accuracy of hybrid meta-GGA density functionals by range separation, J. Phys. Chem. Lett. 2 (2011) 2810–2817.
[59] O.A. Vydrov, G.E. Scuseria, Assessment of a long range corrected hybrid functional, J. Chem. Phys. 125 (2006) 234109-1–234109-9.
[60] S. Grimme, Semiempirical GGA-type density functional constructed with a long range dispersion correction, J. Comput. Chem. 27 (2006) 1787–1799.
[61] J.P. Foster, F. Weinhold, Natural hybrid orbitals, J. Am. Chem. Soc. 102 (1980) 7211–7218.
[62] A.E. Reed, R.B. Weinstock, F. Weinhold, Natural population analysis, J. Chem. Phys. 83 (1985) 735–746.
[63] K. Rajput, V. Kumar, S. Thomas, M.A. Zaeem, D.R. Roy, Ca2C MXene monolayer as a superior anode for metal-ion batteries, 2D Mater. 8 (2021) 35015.
[64] A. Yadav, A. Dashora, N. Patel, A. Miotello, M. Press, D.C. Kothari, Study of 2D MXene Cr2C material for hydrogen storage using density functional theory, Appl. Surf. Sci. 389 (2016) 88–95.
[65] R. Rahimi, M. Solimannejad, Sensing ability of 2D Al2C monolayer toward toxic pnictogen hydrides: a first-principles perspective, Sensor Actuator Phys. 28 (2021), 113000.
[66] U. Yorulmaz, İ. Demiroğlu, D. Çakir, O. Gülseren, C. Sevik, A systematical ab-initio review of promising 2D MXene monolayers towards Li-ion battery applications, J. Phys.: Energy 2 (2020) 32006.
[67] H. Shin, S. Kang, J. Koo, H. Lee, J. Kim, Y. Kwon, Cohesion energetics of carbon allotropes: quantum Monte Carlo study, J. Chem. Phys. 140 (2014), 114702.
[68] A. Fleurence, R. Friedlein, T. Ozaki, H. Kawai, Y. Wang, Y. Yamada-Takamura, Experimental evidence for epitaxial silicene on diboride thin films, Phys. Rev. Lett. 108 (2012), 245501.
[69] S. Li, Semiconductor Physical Electronics, Springer, Berlin, 2006.
[70] Y.H. Zhang, Y.B. Chen, K.G. Zhou, et al., Nanotechnology 20 (2009) 185504–185512.
[71] J. Kong, N.R. Franklin, C. Zhou, M.G. Chapline, S. Peng, K. Cho, H. Dai, Science 287 (2000) 622.